High-energy angle resolved reflection spectroscopy on three-dimensional photonic crystals of self-organized polymeric nanospheres

S. Schutzmann[1]*, I. Venditti[2], P. Prosposito[1], M. Casalboni[1] and M.V. Russo[2]

[1]*Physics Department, University of Rome Tor Vergata and INSTM, via della Ricerca Scientifica 1, 000133 Rome, Italy*

[2] *Chemistry Department, University of Rome La Sapienza, piazzale Aldo Moro 5, 00185 Rome, Italy*

**Corresponding author: schutzmann@roma2.infn.it*

Abstract: We report on the optical characterization of three-dimensional opal-like photonic crystals made by self-organized nanospheres of poly[styrene-(co-2-hydroxyethyl methacrylate)] having a face centred cubic (*fcc*) structure oriented along the [111] direction. A detailed optical characterization of the samples is presented using angle resolved reflection spectroscopy in specular geometry. The investigated energies are between a/λ=0.5 and a/λ=1.5 (where a is the lattice parameter and λ is the light wavelength), a region in which both first and second-order Bragg diffraction are expected. Some interesting features as branching of the Bragg peak dispersion and high energy reflection peaks are revealed. We compare the experimental data with theoretical calculations using both Bragg diffraction and band structure approach. A comparison with recent results reported in the literature is also presented.

OCIS codes: (050.5298) Photonic crystals; (160.1245) Artificially engineered materials; (160.5470) Polymers; (260.1960) Diffraction theory.

References and links

1. E. Yablonovitch, "Inhibited spontaneous emission in solid-state physics and electronics," Phys. Rev. Lett. **58**, 2059-2062 (1987).
2. S. John, "Strong localization of photons in certain disordered dielectric superlattices," Phys. Rev. Lett. **58**, 2486-2489 (1987).
3. G. Pan, R. Kesavamoorthy and S.A. Asher, "Optically nonlinear Bragg diffracting nanosecond optical switches," Phys. Rev. Lett. **78**, 3860-3863 (1997).
4. K. Vynck, D. Cassagne and E. Centeno, "Superlattice for photonic band gap opening in monolayers of dielectric spheres," Opt. Express **14**, 6668-6674 (2006).
5. Y. Nishijima, K. Ueno, S. Joudkazis, V. Mizeikis, H. Misawa, T. Tanimura and K. Maeda, "Inverse silica opal photonic crystal for optical sensing applications," Opt. Express **15**, 12979-12988 (2007).
6. O. Painter, R. K. Lee, A. Scherer, A. Yariv, J. D. O'Brien, P. D. Dapkus and I. Kim, "Two-dimensional photonic band-gap defect mode laser," Science **284**, 1819-1821 (1999).
7. H. Kosaka, T. Kawashima, A. Tomita, M. Notomi, T. Tamamura, T. Sato and S. Kawakami, "Superprism phenomena in photonic crystals," Phys. Rev. B **58**, R10096-R10099 (1998).
8. V. Yannopapas, N. Stefanou and A. Modinos, "Theoretical analysis of the photonic band structure of face-centred cubic colloidal crystals," J. Phys.: Condens. Matter **9**, 10261-10270 (1997).
9. E. Pavarini, L.C. Andreani, C. Soci, M. Galli, F. Marabelli and D. Comoretto, "Band structure and optical properties of opal photonic crystals," Phys. Rev. B **72**, 045102 1-9 (2005).
10. M. Botey, M. Maymó and J. Martorell, "Band-structure determination for finite 3-D photonic crystals," Appl. Phys. B **81**, 277-281 (2005).
11. A. Balestreri, L.C. Andreani and M. Agio, "Optical properties and diffraction effects in opal photonic crystals," Phys. Rev. E **74**, 036603 1-8 (2006).
12. L.A. Dorado, R.A. Depine and H. Míguez, "Effect of extinction on the high-energy optical response of photonic crystals," Phys. Rev. B **75**, 241101(R) 1-4 (2007).

#88898 - $15.00 USD Received 22 Oct 2007; revised 10 Dec 2007; accepted 25 Dec 2007; published 10 Jan 2008

13. A. Reynolds, F. López-Tejeira, D. Cassagne, F.J. García-Vidal, C. Jouanin and J. Sánchez-Dehesa, "Spectral properties of opal-based photonic crystals having a SiO_2 matrix," Phys. Rev. B **60**, 11422-11426 (1999).
14. H.M. van Driel and W.L. Vos, "Multiple Bragg wave coupling in photonic band-gap crystals," Phys. Rev. B **62**, 9872-9875 (2000).
15. Y.A. Vlasov, M. Deutsch and D.J. Norris, "Single-domain spectroscopy of self-assembled photonic crystals," Appl. Phys. Lett. **76**, 1627-1629 (2000).
16. S.G. Romanov, T. Maka, C.M. Sotomayor Torres, M. Müller, R. Zentel, D. Cassagne, J. Manzanares-Martinez and C. Jouanin, "Diffraction of light from thin-film polymethylmetacrylate opaline photonic crystals," Phys. Rev. E **63**, 056603 1-5 (2001).
17. J.F. Galisteo-López and W.L. Vos, "Angle-resolved reflectivity of single-domain photonic crystals: Effects of disorder," Phys. Rev. E **66**, 036616 1-5 (2002).
18. J.F. Galisteo-López, E. Palacios-Lidón, E. Castillo-Martínez and C. López, "Optical study of the pseudogap in thickness and orientation controlled artificial opals," Phys. Rev. B **68**, 115109 1-8 (2003).
19. F. García-Santamaría, J.F. Galisteo-López, P.V. Braun and C. López, "Optical diffraction and high-energy features in three-dimensional photonic crystals," Phys. Rev. B **71**, 195112 1-5 (2005).
20. J.F. Galisteo-López, M. Galli, M. Patrini, A Balestreri, L.C. Andreani and C. López, "Effective refractive index and group velocity determination of three-dimensional photonic crystals by means of white light interferometry," Phys. Rev. B **73**, 125103 1-9 (2006).
21. A.V. Baryshev, A.B. Khanikaev, H. Uchida, M. Inoue and M.F. Limonov, "Interaction of polarized light with three-dimensional opal-based photonic crystals," Phys. Rev. B **73**, 033103 1-4 (2006).
22. S. Wong, V. Kitaev and G.A. Ozin, "Colloidal crystal films: Advances in universality and perfection," J. Am. Chem. Soc. **125**, 15589-15598 (2003).
23. K. Wostyn, Y. Zhao, G. de Schaetzen, L. Hellemans, N. Matsuda, K. Clays and A. Persoons, "Insertion of two-dimensional cavity into a self-assembled colloidal crystal," Langmuir **19**, 4465-4468 (2003).
24. A. Chiappini, C. Armellini, A. Chiasera, M. Ferrari, Y. Jestin, M. Matterelli, M. Montagna, E. Moser, G. Nunzi Conti, S. Pelli, G.C. Righini, M. Clara Gonçalves and R.M. Almeida, "Design of photonic structures by sol-gel-derived silica nanospheres," J. Non-Cryst. Solids **353**, 674-678 (2007).
25. O.L.J. Pursiainen, J.J. Baumberg, H. Winkler, B. Viel, B. Spahn and T. Rhul, "Nanoparticle-tuned structural color from polymer opal," Opt. Express **15**, 9553-9561 (2007)
26. J.F. Galisteo, F. García-Santamaría, D. Golmayo, B.H. Juárez, C. López and E. Palacios, "Self-assembly approach to optical metamaterials," J. Opt. A: Pure Appl. Opt. **7**, S244-S254 (2005).
27. H. Míguez, V. Kitaev and G.A. Ozin, "Band spectroscopy of colloidal photonic crystal films," Appl. Phys. Lett. **84**, 1239-1241 (2004).
28. C. López, "Materials aspects of photonic crystals," Adv. Mater. **15**, 1679-1704 (2003).
29. C. Reese and S. Asher, "Emulsifier-free emulsion polymerization produces highly charged, monodisperse particles for near infrared photonic crystals," J. Colloid Interface Sci. **248**, 41-46 (2002).
30. M. Okubo, T. Suzuki and Y. Fukuhara, "Estimation of heterogeneous surface structure of submicron-sized, composite polymer particles consisting of hydrophobic and hydrophilic components by atomic force microcopy," Colloid. Polym. Sci. **281**, 569-574 (2003).
31. N.W. Ashcroft and N.D. Mermin, *Solid State Physics*, (Saunders, New York, 1976).
32. K. Wostyn, Y. Zhao, B. Yee, K Clays, A. Persoons, G. de Schaetzen and L. Hellemans, "Optical properties and orientation of arrays of polystyrene spheres deposited using convective self-assembly," J. Chem. Phys. **118**, 10752-10757 (2003).
33. J.F. Galisteo-López and C. López, "High-energy optical response of artificial opals," Phys. Rev. B **70**, 035108 1-6 (2004).
34. W.L. Vos and H.M. van Driel, "Higher order Bragg diffraction by strongly photonic *fcc* crystals: onset of a photonic bandgap," Phys. Lett. A **272**, 101-106 (2000).
35. M. Egen and R. Zentel, "Surfactant-free emulsion polymerization of various methacrylates: towards monodisperse colloids for polymer opals," Macromol. Chem Phys. **205**, 1479-1488 (2004).
36. I. Venditti, PhD Thesis (University of Rome La Sapienza, 2007).
37. H. Fujiwara, *Spectroscopic Ellipsometry: Principles and Applications* (Wiley, Chichester, 2007).
38. S. Middleman and A.K. Hochberg, *Process Engineering Analysis in Semiconductor Device Fabrication*, (McGraw-Hill, New York, 1993)
39. S. Bosch, J. Ferré-Borrull and J. Sancho-Parramon, "A general-purpose software for optical characterization of thin films: specific features for microelectronic applications," Solid State Elec. **45**, 703-709 (2001).
40. P. Jiang, G.N. Ostojic, R. Narat, D.M. Mittleman and V.L. Colvin, "The fabrication and bandgap engineering of photonic multilayers," Adv. Mater. **13**, 389-393 (2001).
41. http://ab-initio.mit.edu/mpb/.
42. S.G. Johnson and J.D. Joannopoulos, "Bloch-iterative frequency-domain methods for Maxwell's equations in a planewave basis," Opt. Express **8**, 173-190 (2001).

#88898 - $15.00 USD Received 22 Oct 2007; revised 10 Dec 2007; accepted 25 Dec 2007; published 10 Jan 2008

1. Introduction

Photonic Crystals (PhCs) are engineered structured materials which present a periodic modulation of the dielectric constant on a scale of the order of the optical wavelength. Since the first proposals suggested by Yablonovitch [1] and John [2] in 1987 ever growing interest towards this kind of metamaterials has been addressed. In the last years three-dimensional (3D) PhCs have been widely investigated both from a theoretical and an applicative point of view. The possibility of using PhCs for applications in optical devices such as optical switches, filters [3], waveguides [4], sensors [5], laser cavity [6] and superprisms [7] has been demonstrated. In addition several theoretical [8-12] and experimental [13-21] works have been recently devoted to a better understanding of the complex interactions between electromagnetic waves and energy bands of PhCs, especially in the high frequency region where multiple diffraction takes place.

Among the different techniques used to fabricate 3D PhCs self-assembly from monodisperse colloidal spheres (mostly silica and polymers) has received great attention for their easy fabrication [22-25]. The technique is based on the well-known ability of monodisperse sub-micrometric spheres to self-organize into an ordered close-packed *fcc* structure with [111] as growing direction [26]. PhCs obtained in such a way are generally known as artificial opals.

The first studies on these materials were mostly focussed on the investigation of the interaction of the light with the artificial crystal by Bragg diffraction. From the analysis of the diffracted light a series of allowed and forbidden energy bands can be extracted which are typical of the specific crystal. Many studies have been reported on the fundamental stop band related to the first order Bragg diffraction of (111) lattice planes. Very recently an ever growing interest has been addressed to the analysis of the optical spectra in the energy region around the second-order stop band, leading to an intense debate [12,19,27] about the origin of the high energy bands present in reflectance and transmission spectra of 3D opal-like PhCs. It is common opinion that the peak (dip) in reflectance (transmittance) measurements occurring in the energy region around $a/\lambda \approx 0.5\text{-}0.7$, related to the Bragg diffraction of (111) planes, can be explained in terms of opening of the pseudogap in the band structure near the L point of the Brillouin zone (BZ) [28]. On the contrary there is not a unique interpretation in the high energy region ($a/\lambda>1$) where the situation becomes more complex with the appearance of many different structures both in reflection and transmission spectra, and where no gaps or pseudogaps open up.

In this work we present a detailed optical characterization of an opal-like 3D PhCs made by sub-micrometric spheres of poly[styrene-(co-2-hydroxyethyl methacrylate)] [29] (P(S/HEMA) in the following). The monodispersed polymeric spheres self-assemble in high-quality large-ordered *fcc* structures with the [111] as growing direction. P(S/HEMA) is a co-polymer which presents some specific properties such as a higher refractive index compared with other widely used polymers and a high hydrophilicity [30], that could be useful for many applications.

We have focused our study on the analysis of angle resolved reflectance measurements in *specular geometry* along the L-U and U-X directions of the reciprocal lattice (i.e. in the (ΓLX) plane [31]). The investigated energies are in the range $a/\lambda=0.5 \div 1.5$, a region in which both first and second-order Bragg diffraction of the (111) planes should take place. We observed different features in the reflectance spectra above $a/\lambda=1$ in particular for wide angles of incidence with respect to the surface normal. Analogous results were reported by Wostyn et al. [32] on polymeric opals but their analysis was based on angle resolved transmittance, and by Galisteo-López et al. [33] using both reflectance and transmittance at normal incidence. Similar investigations, based on *angle resolved specular reflection*, have been performed by Vos et al. [34] but on inverse TiO_2 opals. In this case the high refractive index contrast between air and template material leads to a strong photonic interaction between light and PhC, and allows an easier detection of the Bragg diffraction with respect to polymer structures having a low index contrast. To the best of our knowledge this is the first work on

#88898 - $15.00 USD Received 22 Oct 2007; revised 10 Dec 2007; accepted 25 Dec 2007; published 10 Jan 2008

PhCs made by P(S/HEMA) using angle resolved reflectance measurements in specular geometry, and in a high energy region ($a/\lambda>1$). We discuss our results both in terms of classical Bragg diffraction and numerically calculated band structure also comparing our data with results obtained by other groups.

2. Experimental

P(S/HEMA) beads were synthesized by modified emulsion polymerization technique [35]. A detailed description of the synthesis procedure can be found in Ref. 36. The relative ratio between S and HEMA monomers, was selected among a variety of compositions and 50/1 in volume gave the best results in terms of size uniformity and monodispersion of the nano-beads. Thin opaline films were prepared by spreading few drops of emulsion on glass (BK7) substrates. The sedimentation was performed at controlled temperature (36°C) covering a typical area of 2x2 cm^2 where the beads self-assemble in a *fcc* package with the [111] growth direction perpendicular to the substrate plane. Under eye inspection the samples show, for some specific angles, a pronounced opalescence indicating the high order of orientation of the spheres. Scanning Electron Microscopy (SEM) analysis have demonstrated the ordering of the opal structures which presented large ordered mono-crystalline domains extending approximately over hundreds of micrometers, as showed in Fig.1. The sphere diameter, estimated by SEM measurements, was about 330 nm which corresponds to a lattice parameter a = 467 nm.

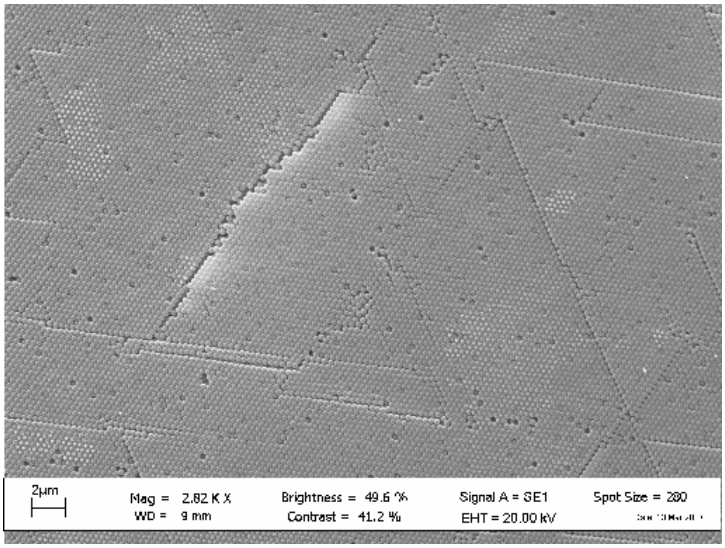

Fig. 1. SEM image of one sample showing the high hexagonal order of the surface. The sphere diameter was estimated to be 330 nm.

Spectroscopic Ellipsometry (SE) [37] was employed to obtain information on thickness of the opaline films and refractive index of the P(S/HEMA) beads. We used a Variable Angle Spectroscopic Ellipsometer (VASE® by J.A. Woollam Co.) in rotating analyzer configuration equipped with a computer controlled compensator which allows measurements of the ellipsometric angles Ψ and Δ in the whole range 0-360° without ambiguity. Focussing probes were used to restrict the investigated area and to reduce undesired effects related to thickness non-uniformity. From the analysis of SE measurements on the opal structures, average thickness of about 7.2 µm was found. Considering the geometry of the structure (*fcc* package grown along the [111] direction) and the sphere diameter measured by SEM images, we have estimated that PhC thickness was composed of about 26-27 monolayers. Finite size effects

#88898 - $15.00 USD Received 22 Oct 2007; revised 10 Dec 2007; accepted 25 Dec 2007; published 10 Jan 2008

can be neglected for such thickness: the structure can be considered as an infinite crystal concerning energy and spectral width of the photonic gap [18].

In order to measure the refractive index of P(S/HEMA) spheres we proceeded as follows. We dissolved the nanospheres in chloroform and we spun the polymeric solution onto glass (BK7) substrates via standard spin-coating deposition technique [38]. The resulting thin films were measured by SE at three different incident angles (namely 55°, 60° and 65°) and the refractive index dispersion was extracted in the wavelength range 300-900 nm. In Fig. 2 is reported the refractive index dispersion for the polymeric film (black line). We assumed that the refractive index of P(S/HEMA) spheres was the same of P(S/HEMA) polymeric films.

The measured refractive index of the polymer was used to estimate the effective refractive index (n_{eff}) of the *fcc* opal structure using a linear *effective medium approximation* (EMA) model [39]:

$$n_{eff}^2 = (1-f)\cdot n_{air}^2 + f\cdot n_{P(S/HEMA)}^2 \qquad (1)$$

where n_{air} and $n_{P(S/HEMA)}$ are the refractive index of air and P(S/HEMA), respectively. f is the sphere filling fraction, that for an ideal close packed *fcc* structure is 0.74. The dispersion of the estimated n_{eff} is reported in Fig. 2.

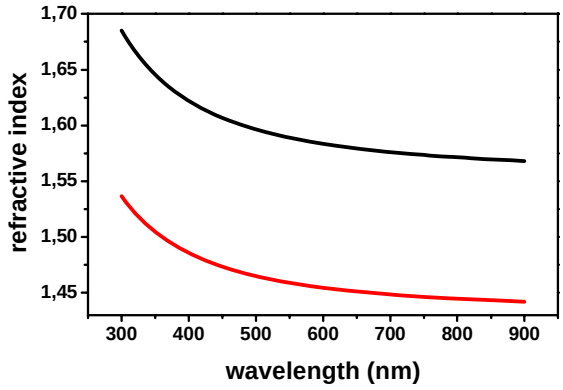

Fig. 2. Refractive index dispersion of P(S/HEMA) material measured by SE (black line). Refractive index dispersion for *fcc* opal PhC calculated using Eq.(1) (red line).

Angular resolved reflectance measurements were performed using the same VASE apparatus. In this case the ellipsometer has been used as a variable angle reflectometer, using the exciting beam with fixed polarization. The angular dependence of the reflected features was studied changing the angle of incidence θ between the light beam and the normal to the crystal surface in the range 20°-70°. The apparatus works in specular geometry, i.e. the detector was placed at 2θ with respect to the light beam when the angle between the incoming beam and the normal to the sample surface was θ. Measurements were carried out using *s*-polarized light in the wavelength range 300-900 nm (corresponding to about $0.52<a/\lambda<1.55$). The samples were oriented in such a way that the **k** vector of diffracted light was in the plane going to the Γ, L, U and X points of the *fcc* BZ of the reciprocal space. We used both focussed beam (where the spot diameter at normal incidence was about 0.2 mm) and coarse beam (spot diameter of about 2 mm) for sample investigation. No difference was found in the reflected spectra indicating a small overall disorientation of domains in the samples. An UV-VIS spectrophotometer (Lambda15 by Perkin-Elmer) was also employed to acquire transmittance spectra at normal incidence.

#88898 - $15.00 USD Received 22 Oct 2007; revised 10 Dec 2007; accepted 25 Dec 2007; published 10 Jan 2008

3. Angle resolved reflection spectroscopy

Figure 3 shows the transmission spectrum at normal incidence performed on a representative sample. The dip at $\lambda \approx 775$ nm is ascribed to the Bragg diffraction of the (111) family of planes. Making reference to photonic band structure language, the dip is related to the opening of the pseudogap between the second and third photonic bands near the L point of the BZ. An important characteristic of opal PhCs is the relative stop-band width, defined as $\Delta E_{gap}/E_{0.}$ Here E_0 is the energy of the transmission dip and ΔE_{gap} full width at half minimum (FWHM) of the spectral band. From Fig. 3 we obtained a relative stop-band width of 0.074 which is in good agreement with the results found by other authors on structures with similar refractive index contrast [40].

At high energy, in the wavelength range below 450 nm, a strong decrease in transmission with many structures can be observed. In this region the second order Bragg diffraction of (111) and (222) planes is expected. In addition theoretical calculations predict that the band structure for such high energies becomes very complicated with a strong intermixture of flat bands leading to perturbations such as splittings and anticrossings [33], that make the interpretation of experimental features rather difficult. Furthermore a recent work by Dorado et al. [12] has shown that the optical extinction related to intrinsic defects of real 3D PhCs has a strong impact on the shape of the experimental spectra, especially at the high frequencies. A full understanding of the physical origins of the experimental observations at the energies above the fundamental pseudogap is still a challenge and is currently a subject of debate [12,19,27,33].

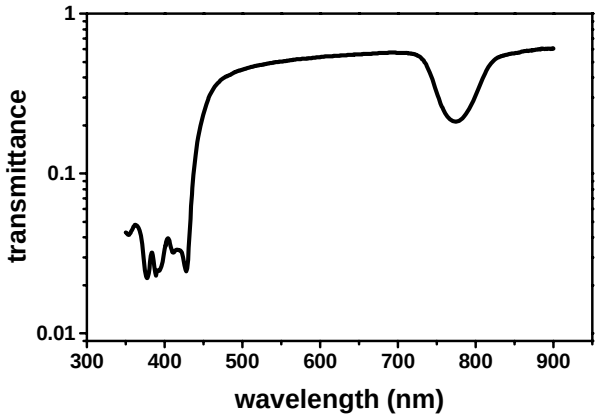

Fig. 3. Transmission spectrum at normal incidence for a P(S/HEMA) PhC.

In order to clarify this point we performed some angle resolved reflectance measurements with high resolution on polymeric PhCs extended in the high energy side up to $a/\lambda = 1.5$. Figure 4 shows the normalized reflectance spectrum of the P(S/HEMA) PhC collected in specular geometry with an angle of incidence of 20°. In addition to the intense Bragg peak of the (111) planes located at λ=750 nm (P1 in the following), two other peaks can be clearly observed at $\lambda = 446$ nm (P2) and λ=392 nm (P3). As the incidence angle θ becomes larger a number of weak, overlapped peaks can be detected in the wavelength region around 400-600 nm. Increasing the incidence angle P1 and P3 peaks shift towards shorter wavelengths while P2 moves in the opposite direction. This behaviour can be appreciated in Fig. 5 where the reflectance spectra for incident angles between 20° and 70° are reported. The spectra are shifted along the intensity axis for clarity while the dash-dotted lines help the reader to follow the evolution of the peak positions.

#88898 - $15.00 USD Received 22 Oct 2007; revised 10 Dec 2007; accepted 25 Dec 2007; published 10 Jan 2008

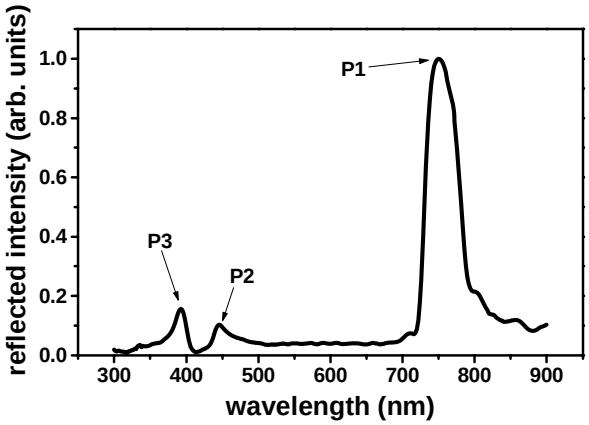

Fig. 4. Normalized reflectance spectrum taken with an angle of incidence $\theta = 20°$. Three peaks centred at λ=750 nm (P1), λ=446 nm (P2) and λ=392 nm (P3) can be clearly observed.

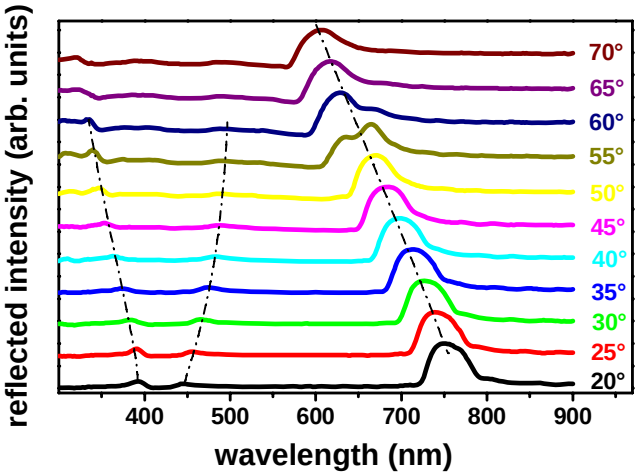

Fig. 5. Angle resolved reflectance spectra for incident angle between 20° (bottom) and 70° (top). The spectra are shifted along the intensity axis for clarity.

Both energy position and shift versus incident angle for P3 and P2 can be well described in terms of the simple Bragg theory if we consider the effect of diffraction by (222) and (220) set of planes, respectively. This aspect will be discussed below in detail. Another significant aspect to be underlined is the splitting of P1 when the incident angle is near 55°. Figure 6 shows more detailed measurements of this double structure taken with 1° step. A new peak at $\lambda \approx 630$ nm (P4 in the following) appears for $\theta \approx 53°$. The spectral positions of P1 and P4 peaks do not change significantly in the selected angle range, but their relative intensity varies as a function of incident angle: for larger θ P4 dominates while P1 tends to disappear. The observation of this feature, attributed to a simultaneous diffraction by the (111) and (200) sets of planes [14,16,18,21], evidences the high quality of our samples, notwithstanding the weak refractive index contrast typical of our polymer-based PhCs.

#88898 - $15.00 USD Received 22 Oct 2007; revised 10 Dec 2007; accepted 25 Dec 2007; published 10 Jan 2008

Many of the experimental results reported above can find an adequate explanation in the frame of the classical Bragg diffraction approach. In this contest the peak wavelength of light diffracted by the (*hkl*) family of planes can be written as [16]:

$$\lambda_{(hkl)} = 2 \cdot d_{(hkl)} \cdot n_{eff} \sqrt{1 - sin^2 r_{(hkl)}} \qquad (2)$$

where $d_{(hkl)}$ is the distance between (*hkl*) planes, $r_{(hkl)}$ is the *internal* angle between wave vector and [*hkl*] direction, and n_{eff} is the effective refractive index of the system that can be obtained by Eq.(1).

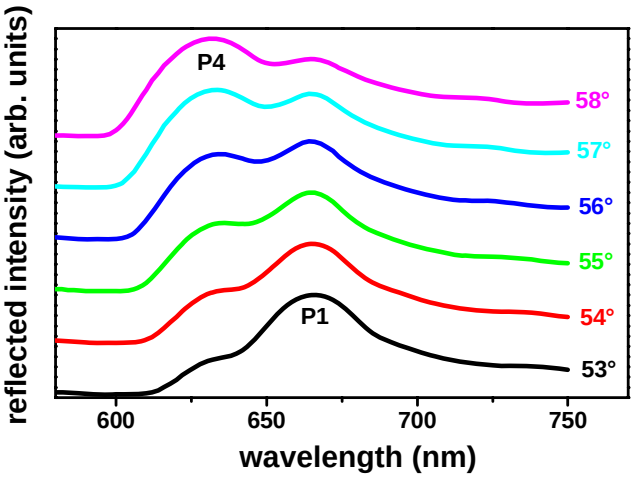

Fig. 6. Peak splitting with avoided crossing for incident angles between 53° and 58°. In addition to P1, a new peak (P4) appears at lower wavelengths. For larger θ P1 tends to disappear and only P4 remains.

Making use of Snell law and knowing the angle between different sets of planes, it is possible to write Eq.(2) as a function of *external* angle between wave vector and [111] direction (i.e. $\theta_{(111)}$) that is the only angle accessible from experimental set-up. In Fig. 7 are reported the wavelengths of the four main peaks observed in the reflectance spectra as a function of the incidence angle θ, and the theoretical Bragg diffractions from (111), (200), (220) and (222) sets of planes. It has to be noted that in Eq.(2), the wavelength dispersion of n_{eff}, as a function of the wavelength, was taken into account making use of the SE data reported in Fig. 2. Moreover, the exact energy positions of P1 and P4 around 55° were obtained by a deconvolution of the reflectance spectra of Fig. 6 using two Gaussians curves. A good agreement between experimental and calculated values, over the entire range of investigated angles, is found.

However, a careful analysis suggests that the Bragg approach fails in a full explanation of the light-opal interaction. In particular the agreement is quite poor near the crossing point of the curves of (111) and (200) sets of planes ($\theta \approx 55°$) where the experimental data reveal an avoided crossing behaviour. In addition the reason why (200) planes diffraction (P4) can be experimentally observed only near the crossing point, while diffraction by (220) planes (P2) is detected in a much wider range is not explained by this simplified model. For these reasons we decided to perform a full band structure calculation of the 3D opal PhC.

#88898 - $15.00 USD Received 22 Oct 2007; revised 10 Dec 2007; accepted 25 Dec 2007; published 10 Jan 2008

Band structure calculations were carried out using the freely available [41] software, developed at MIT, based on a plane wave approach in the frequency domain. Further details about the numeric algorithm can be found in Ref. 42. Since the software does not allow to insert refractive index dispersion of the materials in the calculation we used a mean value of the refractive index that can give adequate results only for short energy ranges, or for materials with low dispersion. In our case the refractive index of the sphere shaped material varies from about 1.58 (at $a/\lambda \approx 0.6$) to about 1.65 (at $a/\lambda \approx 1.5$) and the choice of a single unique average index could lead to noticeable inaccuracies. For these reasons, we decided to use different refractive indexes for different set of calculated bands depending on the energy range of each band. This approach should not present drawbacks when applied to region where the bands are moderately flat, as in our case.

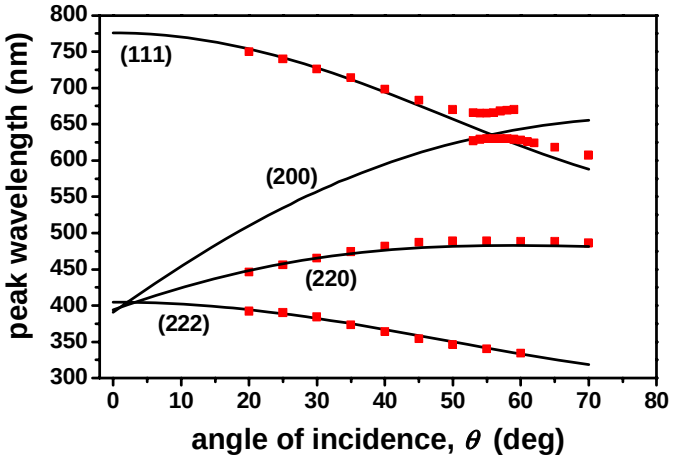

Fig. 7. θ-dependency of the four main peaks wavelengths reported in Fig. 5 and Fig. 6 (red squares). Solid lines indicate the Bragg law predictions for diffraction by (111), (200), (220) and (222) sets of planes using Eq. (2).

Figure 8 shows the calculated band structure (solid lines) of P(S/HEMA) opal PhC along the Γ-L, L-U and U-X directions of the reciprocal space for reduced frequency in the range $0.5<a/\lambda<1.55$. The energy value of the experimental peaks detected in reflectance spectra have been superimposed to the band structure as red squares. The qualitative agreement between theory and experiment for the reflectance peak relative to diffraction by (111) planes (squares at lower energy in the figure) is quite good, even near the U point of the BZ. In addition the band structure calculations account for the peak splitting observed in the experimental spectra near $\theta \approx 55°$. In this context, the reflectance peak is attributed to the opening of a (pseudo)gap in the band structure along the Γ-L direction of the reciprocal space. This leads to a region where no photonic states are available and consequently transmission through the sample is not allowed. The behaviour of the energy bands at higher energy is different since in these cases no (pseudo)gaps open up, and there are always available states. Nevertheless, we observed peaks in reflectance which qualitatively follow the evolution of the energy bands.

#88898 - $15.00 USD Received 22 Oct 2007; revised 10 Dec 2007; accepted 25 Dec 2007; published 10 Jan 2008

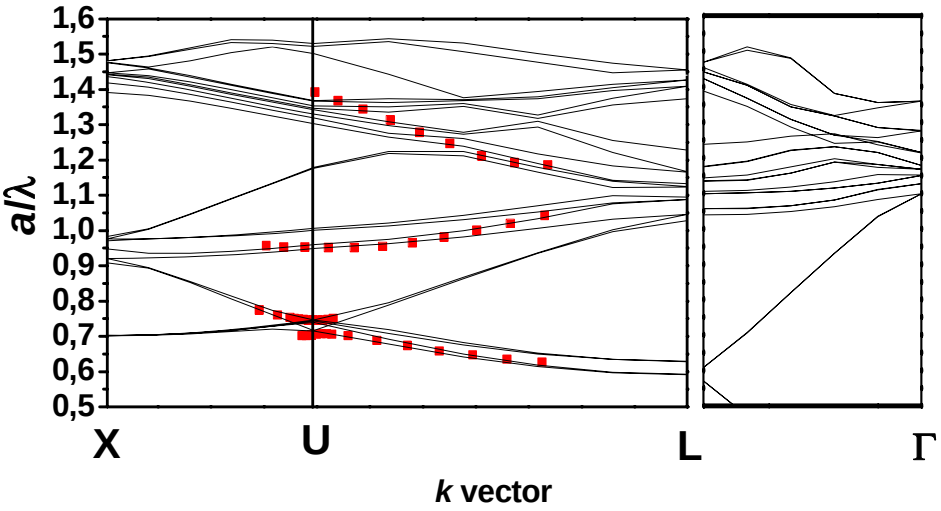

Fig. 8. Photonic band structure (solid lines) of P(S/HEMA) opal PhCs along Γ-L, L-U and U-X directions of the reciprocal space. The red squares are the experimental peaks observed in the angle resolved reflectance spectra.

Different mechanisms can be invoked to explain the high energy bands measured in reflectance. Galisteo-López et al. [33] proposed that band perturbations such as splittings and anticrossings can be related to interaction between bands of similar energy. On the other hand Míguez et al. [27] proposed that for energy bands having low dispersity as a function of the wavevector **k**, the divergence of the effective refractive index ($n_{eff} = c/(\partial\omega/\partial k)$, where c is the speed of light in vacuum) can lead to a high reflectivity of the sample. Our experimental results, obtained by specular reflectance measurements, seem to confirm this latter hypothesis. In fact, in our samples the energy bands above the pseudogap are rather unperturbed and quite flat giving rise to the observed reflectance peaks at high energies in agreement with the mechanism proposed by Míguez et al.

Nevertheless, an exhaustive understanding of the complex phenomena occurring in the interaction between light and 3D PhCs at high energies is still a challenge. Other measurements and calculations should be necessary in order to definitely verify the hypothesis.

4. Conclusions

In summary, we have fabricated high quality 3D opal PhCs via self-assembling of polymeric nanospheres. The material consist of poly[styrene-(co-2-hydroxyethyl methacrylate)], P(S/HEMA), colloidal particles almost monodispersed and synthesized by modified emulsion polymerization technique. A detailed optical characterization of the samples was carried out using angle resolved reflection spectroscopy in specular geometry. The high optical quality of the structures allowed to observe some interesting features such as branching of the Bragg peak dispersion and high energy reflection peaks.

The discussion of the experimental data in terms of both Bragg diffraction approach and photonic band structure calculations is presented. Good agreement between calculated bands and experimental results was found. The detection of reflected peaks in specular geometry at energies above $a/\lambda=1$, where no pseudogaps open up and where the bands are flat but quite unperturbed, seems to suggest that the opal PhCs are effectively characterized by a high value

#88898 - $15.00 USD Received 22 Oct 2007; revised 10 Dec 2007; accepted 25 Dec 2007; published 10 Jan 2008

of reflectivity resulting from a low dispersity of the energy bands, as proposed by Míguez et al. [27].

Acknowledgements

This work was partially supported by Italian Ministero della Università e della Ricerca by Firb 2003 project no. RBNE033KMA ("Composti molecolari e materiali ibridi nanostrutturati con proprietà ottiche risonanti per dispositivi fotonici").

#88898 - $15.00 USD Received 22 Oct 2007; revised 10 Dec 2007; accepted 25 Dec 2007; published 10 Jan 2008